Structural Engineering and Mechanics, *Vol. 62, No. 4 (2017) 401-415*
DOI: https://doi.org/10.12989/sem.2017.62.4.401

A novel and simple HSDT for thermal buckling response of functionally graded sandwich plates

Bouchra Elmossouess*[1], Said Kebdani[1a], Mohamed Bachir Bouiadjra[2a] and Abdelouahed Tounsi[3b]

[1]*Laboratoire de mécanique appliqué, Université des Sciences et Technologie d'ORAN Mouhamed Boudiaf, BP 1505 Elmnouar 31000, ORAN, Algeria*
[2]*Laboratoire des Structures et Matériaux Avancés dans le Génie Civil et Travaux Publics, Université de Sidi Bel Abbes, Faculté de Technologie, Département de génie civil, Algeria*
[3]*Materials and Hydrology Laboratory, University of Sidi Bel Abbes, Faculty of Technology, Civil Engineering Department, Algeria*

(Received September 20, 2016, Revised December 18, 2016, Accepted December 23, 2016)

Abstract. A new higher shear deformation theory (HSDT) is presented for the thermal buckling behavior of functionally graded (FG) sandwich plates. It uses only four unknowns, which is even less than the first shear deformation theory (FSDT) and the conventional HSDTs. The theory considers a hyperbolic variation of transverse shear stress, respects the traction free boundary conditions and contrary to the conventional HSDTs, the present one presents a new displacement field which includes undetermined integral terms. Material characteristics and thermal expansion coefficient of the sandwich plate faces are considered to be graded in the thickness direction according to a simple power-law distribution in terms of the volume fractions of the constituents. The core layer is still homogeneous and made of an isotropic material. The thermal loads are supposed as uniform, linear and non-linear temperature rises within the thickness direction. An energy based variational principle is used to derive the governing equations as an eigenvalue problem. The validation of the present work is carried out with the available results in the literature. Numerical results are presented to demonstrate the influences of variations of volume fraction index, length-thickness ratio, loading type and functionally graded layers thickness on nondimensional thermal buckling loads.

Keywords: thermal buckling; sandwich plate; functionally graded materials; plate theory

1. Introduction

Plates made of functionally graded material (FGM) are widely employed in various branches of engineering such as mechanical, aerospace, chemical, electrical, etc. The main importance of FGM structures and components include high thermal resistance and graded variation of material characteristics along the desired dimension. FGM components like plates are mainly designed for high-temperature environment. FGM components are first introduced for the purpose of employing it as a thermal barrier in aerospace structures. Since then it is gradually employed in various high-temperature applications. Examples include astronautic and aerospace structures like rocket launch pad, space vehicle, aircraft, etc. (Hebali *et al*. 2014, Al-Basyouni *et al*. 2015, Attia *et al*. 2015, Mahi *et al*. 2015, Bourada *et al*. 2015, Ait Atmane *et al*. 2015, Belkorissat *et al*. 2015, Boukhari *et al*. 2016, Kar and Panda 2016a). Recently, various research studies are performed for the thermo-mechanical response of FGM components. For designing FGM plates for application in high-temperature environment, thermal buckling load is an important parameter to be considered. Liew *et al*. (2004) studied the post-buckling and buckling of moderately thick composite plates comprising FG layers under thermal loading. Both perfect and imperfect FG plates are considered, and temperature dependency of material constituents is also included. Na and Kim (2006) presented a finite element approach to study the instability behavior of clamped unsymmetric composite FG plates. In their study, temperature dependency of material properties is also included. Matsunaga (2009) employed a two-dimensional global higher-order deformation theory for thermal buckling of FGM plates. Zhao *et al*. (2009) studied the mechanical and thermal buckling response of FG ceramic-metal plates using the first-order shear deformation plate theory, in conjunction with the Ritz method. Also, Fuchiyama and Noda (1995) examined an FGM plate made of ZrO_2 and Ti 6Al 4V under thermal loading. Piovan and Machado (2011) investigated dynamic stability response of thin-walled FGM beams under axial loading with heat conduction across the thickness. Based on first-order shear deformation theory, Ma and Lee (2011, 2012) examined thermal post-buckling behavior of FG beams under uniform temperature rise using both temperature-dependent (TD) and TID material properties. Kettaf *et al*. (2013) studied the thermal buckling of FG sandwich plates using a new hyperbolic shear displacement model. Duc and Cong (2013) investigated the nonlinear post-buckling of symmetric S-FGM plates resting on elastic foundations using higher order shear deformation plate theory in thermal environments. Tounsi *et al*. (2013) presented a refined trigonometric shear deformation theory

*Corresponding author
E-mail: elmossouessbouchra@yahoo.fr

ISSN: 1225-4568 (Print), 1598-6217 (Online)

for thermo-elastic bending of FG sandwich plates. Bouderba *et al*. (2013) investigated the thermo-mechanical bending response of FG thick plates resting on Winkler-Pasternak elastic foundations. Houari *et al*. (2013) presented a thermo-elastic bending analysis of functionally graded sandwich plates using a new higher order shear and normal deformation theory. Zidi *et al*. (2014) examined the bending behavior of FG plates under hygro-thermo-mechanical loading using a four variable refined plate theory. Ait Amar Meziane *et al*. (2014) presented an efficient and simple refined theory for buckling and free vibration of exponentially graded sandwich plates under various boundary conditions. Bousahla *et al*. (2015) studied thermal stability of plates with functionally graded coefficient of thermal expansion. Bakora and Tounsi (2015) discussed the thermo-mechanical post-buckling response of thick FG plates resting on elastic foundations. Hamidi *et al*. (2015) proposed a sinusoidal plate theory with 5-unknowns and stretching effect for thermo-mechanical bending of FG sandwich plates. Kar *et al*. (2015) presented a nonlinear flexural analysis of laminated composite flat panel under hygro-thermo-mechanical loading. Kar and Panda (2015a) discussed the thermo-elastic behavior of FG doubly curved shell panels using nonlinear finite element method. Akavci (2016) studied the mechanical behavior of FG sandwich plates on elastic foundation. Recently, Laoufi *et al*. (2016) studied the mechanical and hygro-thermal response of FG plates using a hyperbolic shear deformation theory. Bouderba *et al*. (2016) discussed the thermal buckling of FG sandwich plates using a simple shear deformation theory. Beldjelili *et al*. (2016) analyzed the hygro-thermo-mechanical bending of S-FGM plates resting on variable elastic foundations using a four-variable trigonometric plate theory. The nonlinear free vibration behavior of laminated composite shell panels is studied in detail with and without hygrothermal effect by Mahapatra *et al*. (2016a, b, c, d, e, f), Singh and Panda (2015) and Mahapatra and Panda (2015, 2016). The buckling, post-buckling and thermo-mechanical responses of composite structures have been also reported in the open literature (Panda and Singh 2009, 2010a, b, 2011, 2013a, b, c, d, Kar and Panda 2015b, c, 2016b, c, d, Panda and Katariya 2015, Katariya and Panda 2016, Mehar and Panda 2016a, b, 2017, Mehar *et al*. 2016, Kar *et al*. 2016).

It is worth noting that in many of the above mentioned HSDTs as in the CPT or the simple FSDT proposed by Meksi *et al*. (2015) and Bellifa *et al*. (2016), the expression or is present in the displacement field. Consequently, the numerical computation is harder to handle. Normally C1-FEM is required. However, this can be changed if the displacement field is composed with undetermined integral terms as in this article.

In the present investigation, a novel displacement field is developed by considering higher-order distribution of in-plane displacements within the plate thickness and the new constructed displacement field is employed to study the thermal buckling behavior of FG sandwich plates. The use of the integral term in the plate kinematics led to a reduction in the number of unknowns and governing equations. The material characteristics as Young's modulus and thermal expansion coefficient vary according a power law form through-the-thickness coordinate. The governing equations are solved analytically for a FG sandwich plate with simply-supported boundary conditions and subjected to various type of temperature rise. The results based on the hyperbolic theory are compared with those obtained by the higher- and first-order shear deformation plate theories and classical plate theory. The effects of several parameters are discussed.

2. Problem formulation

In this work, a rectangular sandwich plate with uniform thickness h is considered. a and b are the length and the width of the plate, respectively (Fig. 1). The face layers of the sandwich plate are made of an isotropic material with material properties varying smoothly in the z (thickness) direction only. The core layer is made of an isotropic homogeneous material. The vertical positions of the bottom surface, the two interfaces between the core and faces layers, and the top surface are denoted, respectively, by $h_0=-h/2$, h_1, h_2 and $h_3=h/2$. The total thickness of the FG plate is h, where $h=t_C+t_{\mathrm{FGM}}$ and $t_C=h_2-h_1$. t_C and t_{FGM} are the layer thickness of the core and all-FGM layers, respectively.

The effective material properties at the j-th layer of FG plates according to the power-law form are defined by (Belabed *et al*. 2014, Ait Yahia *et al*. 2015, Bounouara *et al*. 2016, Houari *et al*. 2016, Tounsi *et al*. 2016)

$$P^{(j)}(z)=\left(P_c-P_m\right)V^{(j)}(z)+P_m \tag{1}$$

where P_m and P_c are the Young's modulus (E), Poisson's ratio (v) of the bottom and top faces of layer 1 ($h_0 \le z \le h_1$), respectively, and vice versa for layer 3 ($h_2 \le z \le h_3$) depending on the volume fraction $V^{(j)}$ (j=1,2,3). Note that P_m and P_c are, respectively, the corresponding properties of the metal and ceramic of the FG sandwich plate. The volume fraction $V^{(j)}$ of the FGMs is assumed to obey a power-law function along the thickness direction (Houari *et al*. 2011, Bennoun *et al*. 2016)

$$\begin{cases} V^{(1)}(z)=\left(\dfrac{z-h_0}{h_1-h_0}\right)^k & \text{for } z\in\left[h_0,h_1\right] \\ V^{(2)}(z)=1 & \text{for } z\in\left[h_1,h_2\right] \\ V^{(3)}(z)=\left(\dfrac{z-h_3}{h_2-h_3}\right)^k & \text{for } z\in\left[h_2,h_3\right] \end{cases} \tag{2}$$

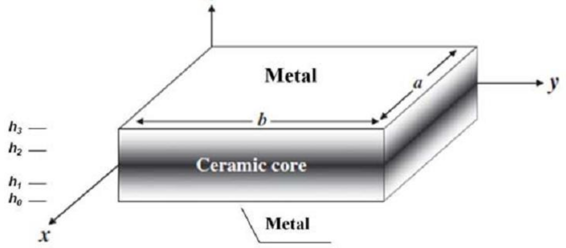

Fig. 1 Geometry of the FGM sandwich plate

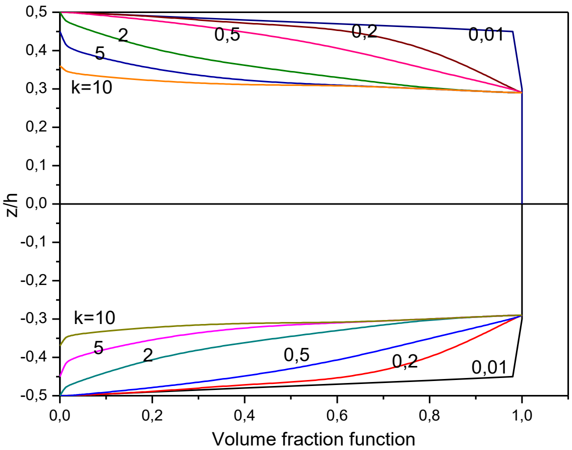

Fig. 2 Variation of volume fraction function through plate thickness for various values of the gradient index k with t_c=0.5h

where k is the power-law exponent, which is non-negative and $z \in \left[-\frac{h}{2}, \frac{h}{2}\right]$. Fig. 2 shows the through-the-thickness variation of the volume fraction function of the ceramic for k=0.01, 0.2, 0.5, 2, 5, and 10. Note that the core of the plate is fully ceramic while the bottom and top surfaces of the plate are metal-rich.

2.1 Kinematics and strains

In this study, the conventional HSDT is modified by considering some simplifying suppositions so that the number of unknowns is reduced. The displacement field of the conventional HSDT is defined by

$$u(x,y,z) = u_0(x,y) - z\frac{\partial w_0}{\partial x} + f(z)\varphi_x(x,y) \tag{3a}$$

$$v(x,y,z) = v_0(x,y) - z\frac{\partial w_0}{\partial y} + f(z)\varphi_y(x,y) \tag{3b}$$

$$w(x,y,z) = w_0(x,y) \tag{3c}$$

Where u_0; v_0; w_0, φ_x, φ_y are five unknown displacements of the mid-plane of the plate, $f(z)$ represents shape function defining the variation of the transverse shear strains and stresses within the thickness. By considering that $\varphi_x = \int \theta(x,y)dx$ and $\varphi_y = \int \theta(x,y)dy$, the Kinematic of the present theory can be expressed in a simpler form as

$$u(x,y,z) = u_0(x,y) - z\frac{\partial w_0}{\partial x} + k_1\, f(z)\int \theta(x,y)\,dx \tag{4a}$$

$$v(x,y,z) = v_0(x,y) - z\frac{\partial w_0}{\partial y} + k_2\, f(z)\int \theta(x,y)\,dy \tag{4b}$$

$$w(x,y,z) = w_0(x,y) \tag{4c}$$

In this study, the shape function is defined by

$$f(z) = \frac{z\cosh\left(\frac{\pi}{2}\right) - \frac{h}{\pi}\sinh\left(\frac{\pi}{h}z\right)}{\cosh\left(\frac{\pi}{2}\right) - 1} \tag{5}$$

It can be seen that the Kinematic in Eq. (4) presents only four unknowns (u_0, v_0, w_0 and θ). The non-linear von Karman strain–displacement equations are as follows

$$\begin{Bmatrix} \varepsilon_x \\ \varepsilon_y \\ \gamma_{xy} \end{Bmatrix} = \begin{Bmatrix} \varepsilon_x^0 \\ \varepsilon_y^0 \\ \gamma_{xy}^0 \end{Bmatrix} + z\begin{Bmatrix} k_x^b \\ k_y^b \\ k_{xy}^b \end{Bmatrix} + f(z)\begin{Bmatrix} k_x^s \\ k_y^s \\ k_{xy}^s \end{Bmatrix}, \quad \begin{Bmatrix} \gamma_{yz} \\ \gamma_{xz} \end{Bmatrix} = g(z)\begin{Bmatrix} \gamma_{yz}^0 \\ \gamma_{xz}^0 \end{Bmatrix}, \tag{6}$$

where

$$\begin{Bmatrix} \varepsilon_x^0 \\ \varepsilon_y^0 \\ \gamma_{xy}^0 \end{Bmatrix} = \begin{Bmatrix} \frac{\partial u_0}{\partial x} + \frac{1}{2}\left(\frac{\partial w_0}{\partial x}\right)^2 \\ \frac{\partial v_0}{\partial x} + \frac{1}{2}\left(\frac{\partial w_0}{\partial y}\right)^2 \\ \frac{\partial u_0}{\partial y} + \frac{\partial v_0}{\partial x} + \left(\frac{\partial w_0}{\partial x}\right)\left(\frac{\partial w_0}{\partial y}\right) \end{Bmatrix}, \quad \begin{Bmatrix} k_x^b \\ k_y^b \\ k_{xy}^b \end{Bmatrix} = \begin{Bmatrix} -\frac{\partial^2 w_0}{\partial x^2} \\ -\frac{\partial^2 w_0}{\partial y^2} \\ -2\frac{\partial^2 w_0}{\partial x \partial y} \end{Bmatrix} \tag{7a}$$

$$\begin{Bmatrix} k_x^s \\ k_y^s \\ k_{xy}^s \end{Bmatrix} = \begin{Bmatrix} k_1\theta \\ k_2\theta \\ k_1\frac{\partial}{\partial y}\int \theta\, dx + k_2\frac{\partial}{\partial x}\int \theta\, dy \end{Bmatrix}, \quad \begin{Bmatrix} \gamma_{yz}^0 \\ \gamma_{xz}^0 \end{Bmatrix} = \begin{Bmatrix} k_1\int \theta\, dy \\ k_2\int \theta\, dx \end{Bmatrix} \tag{7b}$$

and

$$g(z) = \frac{df(z)}{dz} \tag{7c}$$

The integrals used in the above equations shall be resolved by a Navier type method and can be given as follows

$$\frac{\partial}{\partial y}\int \theta\, dx = A'\frac{\partial^2 \theta}{\partial x \partial y}, \quad \frac{\partial}{\partial x}\int \theta\, dy = B'\frac{\partial^2 \theta}{\partial x \partial y}, \quad \int \theta\, dx = A'\frac{\partial \theta}{\partial x}, \quad \int \theta\, dy = B'\frac{\partial \theta}{\partial y} \tag{8}$$

Where the coefficients A' and B' are expressed according to the type of solution used, in this case via Navier. Therefore, A', B', k_1 and k_2 are expressed as follows

$$A' = -\frac{1}{\alpha^2}, \quad B' = -\frac{1}{\beta^2}, k_1 = \alpha^2, k_2 = \beta^2 \tag{9}$$

where α and β are used in expression (20).

It should be noted that unlike the FSDT, this model does not require shear correction coefficients. Moreover, the constitutive relations of a FG sandwich plate can be expressed as

$$\begin{Bmatrix} \sigma_x \\ \sigma_y \\ \tau_{yz} \\ \tau_{xz} \\ \tau_{xy} \end{Bmatrix}^{(j)} = \begin{bmatrix} C_{11} & C_{12} & 0 & 0 & 0 \\ C_{12} & C_{22} & 0 & 0 & 0 \\ 0 & 0 & C_{44} & 0 & 0 \\ 0 & 0 & 0 & C_{55} & 0 \\ 0 & 0 & 0 & 0 & C_{66} \end{bmatrix}^{(j)} \begin{Bmatrix} \varepsilon_x - \alpha T \\ \varepsilon_y - \alpha T \\ \gamma_{xy} \\ \gamma_{yz} \\ \gamma_{xz} \end{Bmatrix}^{(j)} \tag{10}$$

where C_{ij} (i, j=1, 2, 4, 5, 6) are the elastic stiffness of the FG sandwich plate defined by

$$C_{11}^{(j)} = C_{22}^{(j)} = \frac{E^{(j)}(z)}{1-\nu^2}, \quad C_{12}^{(j)} = \frac{\nu E^{(j)}(z)}{1-\nu^2},$$
$$C_{44}^{(j)} = C_{55}^{(j)} = C_{66}^{(j)} = \frac{E^{(j)}(z)}{2(1+\nu)}, \tag{11}$$

and $T(x, y, z)$ is the temperature rise through-the-thickness.

2.2 Stability equations

The equilibrium equations of FG sandwich plates under thermal loadings may be obtained on the basis of the stationary potential energy (Reddy 1984, Bousahla *et al*. 2014, Larbi Chaht *et al*. 2015, Meradjah *et al*. 2015, Nguyen *et al*. 2015, Bourada *et al*. 2016, Draiche *et al*. 2016). The equilibrium equations are deduced as

$$\begin{aligned}
&\delta u_0 : \ \frac{\partial N_x}{\partial x} + \frac{\partial N_{xy}}{\partial y} = 0 \\
&\delta v_0 : \ \frac{\partial N_{xy}}{\partial x} + \frac{\partial N_y}{\partial y} = 0 \\
&\delta w_0 : \ \frac{\partial^2 M_x^b}{\partial x^2} + 2\frac{\partial^2 M_{xy}^b}{\partial x \partial y} + \frac{\partial^2 M_y^b}{\partial y^2} \\
&+ N_x^0 \frac{\partial^2 w_0}{\partial x^2} + 2 N_{xy}^0 \frac{\partial^2 w_0}{\partial x \partial y} + N_y^0 \frac{\partial^2 w_0}{\partial y^2} = 0 \\
&\delta \theta : -k_1 M_x^s - k_2 M_y^s - (k_1 A' + k_2 B')\frac{\partial^2 M_{xy}^s}{\partial x \partial y} \\
&+ k_1 A' \frac{\partial S_{xz}^s}{\partial x} + k_2 B' \frac{\partial S_{yz}^s}{\partial y} = 0
\end{aligned} \tag{12}$$

Using constitutive relations, the stress and moment resultants are defined by

$$\left(N_i, M_i^b, M_i^s\right) = \sum_{j=1}^{3} \int_{h_{j-1}}^{h_j} (1, z, f)\sigma_i^{(j)} dz,$$
$$(i = x, y, xy) \text{ and} \tag{13}$$

$$\left(S_{xz}^s, S_{yz}^s\right) = \sum_{j=1}^{3} \int_{h_{j-1}}^{h_j} g\left(\tau_{xz}, \tau_{yz}\right)^{(j)} dz$$

Upon substitution of Eq. (6) into Eq. (10) and the subsequent results into Eq. (13) the stress resultants are determined in the matrix form as

$$\begin{Bmatrix} N_x \\ N_y \\ N_{xy} \\ M_x^b \\ M_y^b \\ M_{xy}^b \\ M_x^s \\ M_y^s \\ M_{xy}^s \end{Bmatrix} = \begin{bmatrix} A_{11} & A_{12} & 0 & B_{11} & B_{12} & 0 & B_{11}^s & B_{12}^s & 0 \\ A_{12} & A_{22} & 0 & B_{12} & B_{22} & 0 & B_{12}^s & B_{22}^s & 0 \\ 0 & 0 & A_{66} & 0 & 0 & B_{66} & 0 & 0 & B_{66}^s \\ B_{11} & B_{12} & 0 & D_{11} & D_{12} & 0 & D_{11}^s & D_{12}^s & 0 \\ B_{12} & B_{22} & 0 & D_{12} & D_{22} & 0 & D_{12}^s & D_{22}^s & 0 \\ 0 & 0 & B_{66} & 0 & 0 & D_{66} & 0 & 0 & D_{66}^s \\ B_{11}^s & B_{12}^s & 0 & D_{11}^s & D_{12}^s & 0 & H_{11}^s & H_{12}^s & 0 \\ B_{12}^s & B_{22}^s & 0 & D_{12}^s & D_{22}^s & 0 & H_{12}^s & H_{22}^s & 0 \\ 0 & 0 & B_{66}^s & 0 & 0 & D_{66}^s & 0 & 0 & H_{66}^s \end{bmatrix} \begin{Bmatrix} \varepsilon_x^0 \\ \varepsilon_y^0 \\ \gamma_{xy}^0 \\ k_x^b \\ k_y^b \\ k_{xy}^b \\ k_x^s \\ k_y^s \\ k_{xy}^s \end{Bmatrix} - \begin{Bmatrix} N_x^T \\ N_y^T \\ 0 \\ M_x^{bT} \\ M_y^{bT} \\ 0 \\ M_x^{sT} \\ M_y^{sT} \\ 0 \end{Bmatrix} \tag{14a}$$

$$\begin{Bmatrix} S_{yz}^s \\ S_{xz}^s \end{Bmatrix} = \begin{bmatrix} A_{44}^s & 0 \\ 0 & A_{55}^s \end{bmatrix} \begin{Bmatrix} \gamma_{yz}^0 \\ \gamma_{xz}^0 \end{Bmatrix} \tag{14b}$$

$$\begin{Bmatrix} A_{11} & B_{11} & D_{11} & B_{11}^s & D_{11}^s & H_{11}^s \\ A_{12} & B_{12} & D_{12} & B_{12}^s & D_{12}^s & H_{12}^s \\ A_{66} & B_{66} & D_{66} & B_{66}^s & D_{66}^s & H_{66}^s \end{Bmatrix} =$$
$$\sum_{j=1}^{3} \int_{h_{j-1}}^{h_j} C_{11}^{(j)} \left(1, z, z^2, f(z), z\, f(z), f^2(z)\right) \begin{Bmatrix} 1 \\ \nu \\ \frac{1-\nu}{2} \end{Bmatrix} dz \tag{15a}$$

Where stiffness components are expressed as

$$\left(A_{22}, B_{22}, D_{22}, B_{22}^s, D_{22}^s, H_{22}^s\right) = \left(A_{11}, B_{11}, D_{11}, B_{11}^s, D_{11}^s, H_{11}^s\right) \tag{15b}$$

$$A_{44}^s = A_{55}^s = \sum_{j=1}^{3} \int_{h_{j-1}}^{h_j} C_{44}^{(j)} \left[g(z)\right]^2 dz, \tag{15c}$$

The stress and moment resultants, $N_x^T = N_y^T$; $M_x^{bT} = M_y^{bT}$ and $M_x^{sT} = M_y^{sT}$; to thermal loading are defined by

$$\begin{Bmatrix} N_x^T \\ M_x^{bT} \\ M_y^{bT} \end{Bmatrix} = \sum_{j=1}^{3} \int_{h_{j-1}}^{h_j} \frac{E^{(j)}(z)}{1-\nu} \alpha^{(j)} T \begin{Bmatrix} 1 \\ z \\ f(z) \end{Bmatrix} dz \tag{16}$$

In order to determine the stability equations and study the thermal buckling behavior of the FG sandwich plate, the adjacent equilibrium criterion is employed (Brush and Almroth 1975). By using this formulation, the governing stability equations are obtained as

$$\begin{aligned}
&\frac{\partial N_x^1}{\partial x}+\frac{\partial N_{xy}^1}{\partial y}=0\\
&\frac{\partial N_{xy}^1}{\partial x}+\frac{\partial N_y^1}{\partial y}=0\\
&\frac{\partial^2 M_x^{b1}}{\partial x^2}+2\frac{\partial^2 M_{xy}^{b1}}{\partial x\partial y}+\frac{\partial^2 M_y^{b1}}{\partial y^2}+N_x^0\frac{\partial^2 w_0^1}{\partial x^2}+\\
&2N_{xy}^0\frac{\partial^2 w_0^1}{\partial x\partial y}+N_y^0\frac{\partial^2 w_0^1}{\partial y^2}=0\\
&-k_1 M_x^{s1}-k_2 M_y^{s1}-(k_1A'+k_2B')\frac{\partial^2 M_{xy}^{s1}}{\partial x\partial y}+\\
&k_1A'\frac{\partial S_{xz}^{s1}}{\partial x}+k_2B'\frac{\partial S_{yz}^{s1}}{\partial y}=0
\end{aligned}\tag{17}$$

where N_x^0, N_{xy}^0 and N_y^0 are the pre-buckling forces. Eq. (17) can be expressed in terms of displacements (u_0^1, v_0^1, w_0^1, θ^1) by substituting for the stress resultants from Eq. (14). For FG sandwich plate, the governing equations Eq. (17) take the form

$$\begin{aligned}
&A_{11}\frac{\partial^2 u_0^1}{\partial x^2}+A_{12}\frac{\partial^2 v_0^1}{\partial x\partial y}+A_{66}\left(\frac{\partial^2 u_0^1}{\partial y^2}+\frac{\partial^2 v_0^1}{\partial x\partial y}\right)\\
&-B_{11}\frac{\partial^3 w_0^1}{\partial x^3}-B_{12}\frac{\partial^3 w_0^1}{\partial x\partial y^2}-2B_{66}\frac{\partial^3 w_0^1}{\partial x\partial y^2}\\
&+B_{11}^sA'k_1\frac{\partial^3\theta^1}{\partial x^3}\;B_{12}^sB'k_2\frac{\partial^3\theta^1}{\partial x\partial y^2}\\
&+B_{66}^s(A'k_1+B'k_2)\frac{\partial^3\theta^1}{\partial x\partial y^2}=0
\end{aligned}\tag{18a}$$

$$\begin{aligned}
&A_{12}\frac{\partial^2 u_0^1}{\partial x\partial y}+A_{22}\frac{\partial^2 v_0^1}{\partial y^2}+A_{66}\left(\frac{\partial^2 u_0^1}{\partial x\partial y}+\frac{\partial^2 v_0^1}{\partial x^2}\right)\\
&-B_{12}\frac{\partial^3 w_0^1}{\partial x^2\partial y}-B_{22}\frac{\partial^3 w_0^1}{\partial y^3}-2B_{66}\frac{\partial^3 w_0^1}{\partial x^2\partial y}+B_{12}^sA'k_1\frac{\partial^3\theta^1}{\partial x^2\partial y}\\
&B_{22}^sB'k_2\frac{\partial^3\theta^1}{\partial y^3}+B_{66}^s(A'k_1+B'k_2)\frac{\partial^3\theta^1}{\partial x^2\partial y}=0
\end{aligned}\tag{18b}$$

$$\begin{aligned}
&B_{11}\frac{\partial^3 u_0^1}{\partial x^3}+B_{12}\left(\frac{\partial^3 u_0^1}{\partial x\partial y^2}+\frac{\partial^3 v_0^1}{\partial x^2\partial y}\right)+B_{22}\frac{\partial^3 v_0^1}{\partial y^3}\\
&+2B_{66}\left(\frac{\partial^3 u_0^1}{\partial x\partial y^2}+\frac{\partial^3 v_0^1}{\partial x^2\partial y}\right)-D_{11}\frac{\partial^4 w_0^1}{\partial x^4}\\
&-2D_{12}\frac{\partial^4 w_0^1}{\partial x^2\partial y^2}-D_{22}\frac{\partial^4 w_0^1}{\partial y^4}-4D_{66}\frac{\partial^4 w_0^1}{\partial x^2\partial y^2}\\
&+D_{11}^sA'k_1\frac{\partial^4\theta^1}{\partial x^4}+D_{12}^s(A'k_1+B'k_2)\frac{\partial^4\theta^1}{\partial x^2\partial y^2}\\
&+D_{22}^sB'k_2\frac{\partial^4\theta^1}{\partial y^4}+2D_{66}^s(A'k_1+B'k_2)\frac{\partial^4\theta^1}{\partial x^2\partial y^2}\\
&+N_x^0\frac{\partial^2 w_0^1}{\partial x^2}+N_y^0\frac{\partial^2 w_0^1}{\partial y^2}+2N_{xy}^0\frac{\partial^2 w_0^1}{\partial x\partial y}=0
\end{aligned}\tag{18c}$$

$$\begin{aligned}
&-B_{11}^sA'k_1\frac{\partial^3 u_0^1}{\partial x^3}-B_{12}^s\left(A'k_1\frac{\partial^3 v_0^1}{\partial x^2\partial y}+B'k_2\frac{\partial^3 u_0^1}{\partial x\partial y^2}\right)\\
&-B_{22}^sB'k_2\frac{\partial^3 v_0^1}{\partial y^3}-D_{66}\begin{pmatrix}(A'k_1+B'k_2)\dfrac{\partial^3 u_0^1}{\partial x\partial y^2}\\+(A'k_1+B'k_2)\dfrac{\partial^3 v_0^1}{\partial x^2\partial y}\end{pmatrix}+\\
&D_{11}^sA'k_1\frac{\partial^4 w_0^1}{\partial x^4}+D_{12}^s(A'k_1+B'k_2)\frac{\partial^4 w_0^1}{\partial x^2\partial y^2}\\
&D_{22}^sB'k_2\frac{\partial^4 w_0^1}{\partial y^4}+2D_{66}^s(A'k_1+B'k_2)\frac{\partial^4 w_0^1}{\partial x^2\partial y^2}\\
&-H_{11}^s(A'k_1)^2\frac{\partial^4\theta^1}{\partial x^4}-2H_{12}^sA'k_1B'k_2\frac{\partial^4\theta^1}{\partial x^2\partial y^2}\\
&-H_{22}^s(B'k_2)^2\frac{\partial^4\theta^1}{\partial y^4}-H_{66}^s(A'k_1+B'k_2)^2\frac{\partial^4\theta^1}{\partial x^2\partial y^2}\\
&+A_{55}^s(A'k_1)^2\frac{\partial^2\theta^1}{\partial x^2}+A_{44}^s(B'k_2)^2\frac{\partial^2\theta^1}{\partial y^2}=0
\end{aligned}\tag{18d}$$

3. Closed-form solution

Rectangular sandwich plates are generally classified according to the type of support employed. Here, we are concerned with the exact solutions of Eq. (18) for a simply supported FG sandwich plate.

Based on the Navier method, the following expansions of displacements u_0^1; v_0^1; w_0^1 and θ^1 are chosen to automatically satisfy the boundary conditions

$$\begin{Bmatrix}u_0^1\\v_0^1\\w_0^1\\\theta^1\end{Bmatrix}=\sum_{m=1}^{\infty}\sum_{n=1}^{\infty}\begin{Bmatrix}U_{mn}\cos(\alpha x)\sin(\beta y)\\V_{mn}\sin(\alpha x)\cos(\beta y)\\W_{mn}\sin(\alpha x)\sin(\beta y)\\X_{mn}\sin(\alpha x)\sin(\beta y)\end{Bmatrix}\tag{19}$$

where U_{mn}, V_{mn}, W_{mn}, X_{mn} are arbitrary parameters to be determined. α and β are defined as

$$\alpha=m\pi/a\quad\text{and}\quad\beta=n\pi/b\tag{20}$$

Substituting Eq. (19) into Eq. (18), the closed-form solution of buckling load can be obtained from

$$\begin{bmatrix}a_{11}&a_{12}&a_{13}&a_{14}\\a_{12}&a_{22}&a_{23}&a_{24}\\a_{13}&a_{23}&a_{33}+N_x^0\alpha^2+N_y^0\beta^2&a_{34}\\a_{14}&a_{24}&a_{34}&a_{44}\end{bmatrix}\begin{Bmatrix}U_{mn}\\V_{mn}\\W_{mn}\\X_{mn}\end{Bmatrix}=\begin{Bmatrix}0\\0\\0\\0\end{Bmatrix}\tag{21}$$

Where

$$\begin{aligned}
a_{11}&=-(A_{11}\alpha^2+A_{66}\beta^2)\\
a_{12}&=-\alpha\,\beta\,(A_{12}+A_{66})\\
a_{13}&=\alpha(B_{11}\alpha^2+(B_{12}+2B_{66})\beta^2)
\end{aligned}\tag{22}$$

$$a_{14} = -\alpha(B_{11}^s A' k_1 \alpha^2 + B_{12}^s B' k_2 \beta^2 + B_{66}^s (A' k_1 + B' k_2)\beta^2)$$

$$a_{22} = -\alpha^2 A_{66} - \beta^2 A_{22}$$

$$a_{23} = \beta(B_{22}\beta^2 + (B_{12} + 2B_{66})\alpha^2)$$

$$a_{24} = -\beta\left(B_{22}^s B' k_2 \beta^2 + \alpha^2 \left(\begin{array}{l} B_{12}^s A' k_1 \\ + B_{66}^s (A' k_1 + B' k_2) \end{array} \right) \right)$$

$$a_{33} = -\alpha^2 \left(D_{11}\alpha^2 + (2D_{12} + 4D_{66})\beta^2\right) - D_{22}\beta^4$$

$$a_{34} = D_{11}^s A' k_1 \alpha^4 + D_{12}^s (A' k_1 + B' k_2)\beta^2\alpha^2 + D_{22}^s B' k_2 \beta^4 + 2D_{66}^s (A' k_1 + B' k_2)\beta^2\alpha^2$$

$$a_{44} = -(H_{11}^s \alpha^2 k_1 + 2k_1\beta^2 H_{66}^s + 2H_{66}^s \alpha^2 k_2 + H_{12}^s \alpha^2 k_2 + k_1\beta^2 H_{12}^s + k_2\beta^2 H_{22}^s + A_s^{44} k_1 + A_s^{55} k_2)$$

By using the condensation technique to eliminate the axial displacements U_{mn} and V_{mn}, Eq. (21) can be rewritten as

$$\begin{bmatrix} \bar{a}_{33} + N_x^0 \alpha^2 + N_y^0 \beta^2 & \bar{a}_{34} \\ \bar{a}_{43} & \bar{a}_{44} \end{bmatrix} \begin{Bmatrix} W_{mn} \\ X_{mn} \end{Bmatrix} = \begin{Bmatrix} 0 \\ 0 \end{Bmatrix} \tag{23}$$

where

$$\bar{a}_{33} = a_{33} - \frac{a_{13}(a_{13}a_{22} - a_{12}a_{23}) - a_{23}(a_{11}a_{23} - a_{12}a_{13})}{a_{11}a_{22} - a_{12}^2}$$

$$\bar{a}_{34} = a_{34} - \frac{a_{14}(a_{13}a_{22} - a_{12}a_{23}) - a_{24}(a_{11}a_{23} - a_{12}a_{13})}{a_{11}a_{22} - a_{12}^2}$$

$$\bar{a}_{43} = a_{34} - \frac{a_{13}(a_{14}a_{22} - a_{12}a_{24}) - a_{23}(a_{11}a_{24} - a_{12}a_{14})}{a_{11}a_{22} - a_{12}^2} \tag{24}$$

$$\bar{a}_{44} = a_{44} - \frac{a_{14}(a_{14}a_{22} - a_{12}a_{24}) - a_{24}(a_{11}a_{24} - a_{12}a_{14})}{a_{11}a_{22} - a_{12}^2}$$

The system of homogeneous Eq. (23) has a nontrivial solution only for discrete values of the buckling load. For a nontrivial solution, the determinant of the coefficients (W_{mn}, X_{mn}) must equal zero

$$\begin{vmatrix} \bar{a}_{33} + N_x^0 \alpha^2 + N_y^0 \beta^2 & \bar{a}_{34} \\ \bar{a}_{43} & \bar{a}_{44} \end{vmatrix} = 0 \tag{25}$$

The obtained equation may be solved for the buckling load. This gives the following relation for buckling load

$$N_x^0 \alpha^2 + N_y^0 \beta^2 = \frac{\bar{a}_{34}\bar{a}_{43} - \bar{a}_{33}\bar{a}_{44}}{\bar{a}_{44}} \tag{26}$$

In this case, a rectangular sandwich plate subjected to thermal loads is examined.To obtain the critical buckling temperature, the pre-buckling thermal loads should be determined. Hence, solving the membrane form of the equilibrium equations and by using the technique proposed by Meyers and Hyer (1991), the pre-buckling load resultants of FG sandwich plate exposed to the temperature variation within the thickness are found to be

$$N_x^0 = -\sum_{j=1}^{3} \int_{h_{j-1}}^{h_j} \frac{E^{(j)}(z)}{1-\nu} \alpha^{(j)}(z) T(z)\, dz,$$
$$N_y^0 = -\sum_{j=1}^{3} \int_{h_{j-1}}^{h_j} \frac{E^{(j)}(z)}{1-\nu} \alpha^{(j)}(z) T(z)\, dz, \tag{27}$$
$$N_{xy}^0 = 0$$

In this article, to examine the effect of the considered type of temperature variation within the thickness on stability buckling response of FG sandwich plate, three types of thermal loading within the plate thickness are taken.

3.1 Uniform temperature rise (UTR)

It is assumed that the initial uniform temperature of the FG sandwich plate is T_i, and the temperature is uniformly elevated to a final value T_f such that the plate buckles. Thus, the temperature change is

$$T(z) = T_f - T_i = \Delta T \tag{28}$$

By employing the equations (26), (27), and (28) the following equation for thermal buckling load is deduced

$$\Delta T(m,n) = \frac{1}{\alpha^2 + \beta^2} \frac{\bar{a}_{33}\bar{a}_{44} - \bar{a}_{34}\bar{a}_{43}}{\bar{a}_{44}} \frac{1}{\int_{-h/2}^{h/2} \frac{E(z)\, \alpha(z)}{1-\nu} dz} \tag{29}$$

3.2 Linear temperature distribution through the thickness (LTD)

The following linear temperature distribution within the thickness of the FG sandwich plate is considered

$$T(z) = \Delta T\left(\frac{z}{h} + \frac{1}{2}\right) + T_m, \quad \Delta T = T_c - T_m \tag{30}$$

Identically to the UTR procedure, the following expression for thermal buckling load is deduced

$$\Delta T(m,n) = \frac{1}{\int_{-h/2}^{h/2} \frac{E(z)\, \alpha(z)\left(\frac{z}{h} + \frac{1}{2}\right)}{1-\nu} dz} \left(\frac{1}{\alpha^2 + \beta^2} \frac{\bar{a}_{33}\bar{a}_{44} - \bar{a}_{34}\bar{a}_{43}}{\bar{a}_{44}} - \int_{-h/2}^{h/2} \frac{E(z)\, \alpha(z) T_M}{1-\nu} dz \right) \tag{31}$$

3.3 Non-linear temperature distribution through the thickness (NTD)

The following non-linear temperature distribution within the thickness of the FG sandwich plate is considered

$$T(z) = \Delta T\left(\frac{z}{h}+\frac{1}{2}\right)^{\gamma} + T_m, \quad \Delta T = T_c - T_m \tag{32}$$

Identically to the UTR procedure, the following expression for thermal buckling load is deduced

$$\Delta T(m,n) = \frac{1}{\displaystyle\int_{-h/2}^{h/2} \frac{E(z)\,\alpha(z)\left(\frac{z}{h}+\frac{1}{2}\right)^{\gamma}}{1-\nu}\,dz} \left(\frac{1}{\alpha^2+\beta^2}\frac{\bar{a}_{33}\bar{a}_{44}-\bar{a}_{34}\bar{a}_{43}}{\bar{a}_{44}} - \int_{-h/2}^{h/2}\frac{E(z)\,\alpha(z)T_M}{1-\nu}\,dz\right) \tag{33}$$

where γ is the temperature exponent ($0<\gamma<\infty$). Note that the value of γ equal to unity represents a linear temperature change across the thickness. While the value of γ excluding unity represents a non-linear temperature change through-the-thickness.

5. Results and discussion

This section is dedicated to inspect the thermal buckling characteristics of FG sandwich plates under thermal loading. For this purpose, three different functionally graded plate materials are considered for the present study. These are Titanium alloy (Ti–6A1–4V)-Zirconia (ZrO2), Stainless Steel (SUS304)-Silicon Nitride (Si3N4), and Stainless Steel-Alumina (Al2O3) and hereafter, these are referred as FGM 1, FGM 2 and FGM 3 respectively. The material properties of the constituents of these FGMs are given in Table 1. The general formulation presented in the previous sections for the thermal stability analysis of the FG sandwich plates subjected to uniform, linear and non-linear temperature rises through-the-thickness is illustrated in this section using the new HSDT.

The shear correction factor for FSDT is set equal to 5/6. For the linear and non-linear temperature rises through-the-thickness, T_m=25°C.

In Tables 2-4, FGM 1 is considered and comparisons of the critical buckling temperatures difference ($T_{cr}=10^{-3}\Delta T_{cr}$) of FG sandwich plates with those of reported by Kettaf *et al*. (2013) is presented for the uniform, linear and nonlinear cases of temperature distribution within the thickness, respectively. In these tables, critical buckling temperature results are presented for various gradient indices and thickness of the core t_c (ceramic layer) at a/h=5. The results of present work are in good agreement with the previous ones. It can be observed from Tables 2 and 3, that with increasing the gradient index k, the thermal buckling temperatures are reduced. Thus, the reduction in thermal buckling temperature of a FG sandwich plate could be attributed to the metal property. This remark is also confirmed when small gradient indices are considered ($k\leq 2$) for all values of t_c. A small gradient index k shows that the ceramic is the dominant constituent in FG sandwich plates. However, Table 3 demonstrates that the thermal stability temperatures are reduced with decreasing the gradient index k when the plate is subjected to non-linear temperature rise with γ=5. It can be seen that the thermal stability temperature T_{cr} is reduced with increasing the thickness of the core layer (t_c) for all employed index.

Fig. 3 presents the influence of the gradient index on the critical stability temperature T_{cr} of FG sandwich plates under uniform, linear and non-linear temperature change through-the-thickness using the present HSDT. It can be seen from Fig. 3 that the critical stability temperature for the plates under a non-linear temperature variation is higher than that for the plates under uniform temperature variation.

Table 1 Material properties used in the FG sandwich plate

Properties	Ti–6A1–4V	ZrO_2	SUS304	Si_3N_4	Al_2O_3
E (GPa)	66.2	244.27	201.04	348.43	349.55
ν	0.3	0.3	0.3	0.3	0.3
α (10^{-6}/K)	10.3	12.766	12.330	5.8723	6.8269

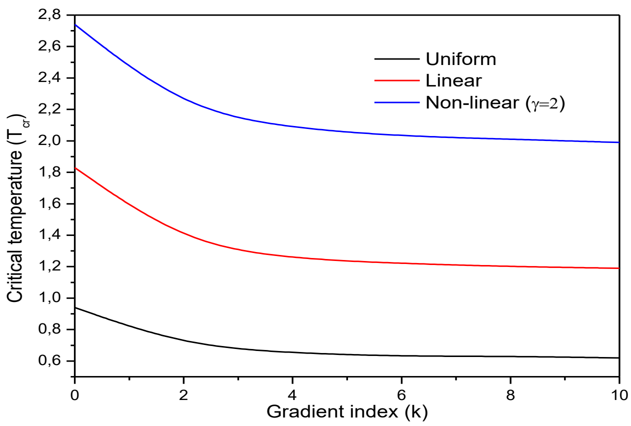

Fig. 3 Critical stability temperature difference T_{cr} of FGM 1 versus the gradient index k for FG sandwich square plate with a/h=10 and t_c=0.6h

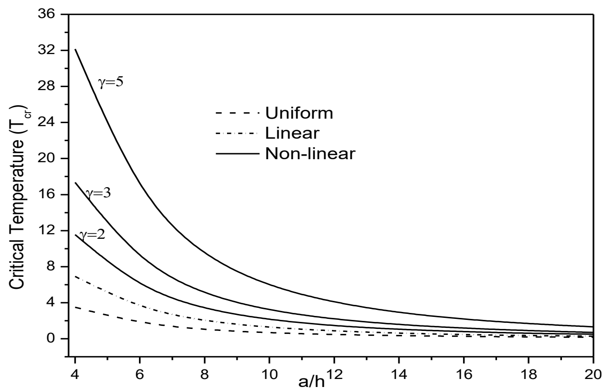

Fig. 4 Critical stability temperature difference T_{cr} of FGM 1 versus the thickness ratio *a/h* for FG sandwich square plate with k=2 and t_c=0.8h

Table 2 Critical buckling temperature T_{cr} of FG sandwich square plates under uniform temperature rise versus gradient index k and t_c/h (a/h=5)

		k						
t_c/h	Theory	0	0.2	0.5	1	2	5	10
0	Present	3.23681	3.07015	2.86983	2.68604	2.62702	2.92887	3.29712
	Ref[a]	3.23720	3.07138	2.87207	2.68975	2.63325	2.93978	3.30959
	SSDT[a]	3.23775	3.071197	2.87277	2.69065	2.63460	2.94205	3.31226
	TSDT[a]	3.23652	3.07042	2.87074	2.68781	2.63018	2.93446	3.30340
	FSDT[a]	3.23493	3.04858	2.83507	2.64222	2.57355	2.86226	3.23289
	CPT[a]	3.96470	3.66606	3.34559	3.06734	2.96200	3.32950	3.82441
0.2	Present	3.23681	3.05449	2.82968	2.59114	2.39414	2.34515	2.41700
	Ref[a]	3.23720	3.05543	2.83135	2.59388	2.39856	2.35252	2.42641
	SSDT[a]	3.23775	3.05598	2.83194	2.59458	2.39953	2.35401	2.42827
	TSDT[a]	3.23652	3.05461	2.83030	2.59241	2.39637	2.34898	2.42195
	FSDT[a]	3.23493	3.03394	2.79675	2.55053	2.34734	2.28926	2.35538
	CPT[a]	3.9647	3.64978	3.30066	2.955338	2.68016	2.59922	2.68195
0.4	Present	3.23681	3.05896	2.84261	2.60446	2.37248	2.19597	2.15439
	Ref[a]	3.23720	3.05915	2.84285	2.60512	2.37406	2.19921	2.17624
	SSDT[a]	3.23775	3.05956	2.84318	2.60545	2.3745	2.19992	2.17714
	TSDT[a]	3.23652	3.05867	2.84246	2.60462	2.3732	2.19763	2.17417
	FSDT[a]	3.23493	3.04171	2.81495	2.57038	2.33409	2.15296	2.12571
	CPT[a]	3.96470	3.66567	3.33354	2.99117	2.67295	2.43609	2.39804
0.5	Present	3.23681	3.07004	2.87034	2.65022	2.42889	2.23857	2.17543
	Ref[a]	3.2372	3.0698	2.86974	2.64965	2.42885	2.23972	2.17737
	SSDT[a]	3.23775	3.07014	2.86992	2.64976	2.429	2.24005	2.17784
	TSDT[a]	3.23652	3.06952	2.86972	2.6497	2.42873	2.2391	2.1764
	FSDT[a]	3.23493	3.05527	2.84659	2.62069	2.39542	2.2013	2.13606
	CPT[a]	3.9647	3.68764	3.38155	3.06366	2.75801	2.50252	2.41816
0.6	Present	3.23681	3.08772	2.91272	2.72089	2.52472	2.34401	2.27490
	Ref[a]	3.2372	3.08713	2.91139	2.71917	2.52309	2.34313	2.27452
	SSDT[a]	3.23775	3.08741	2.91146	2.71909	2.52297	2.3431	2.27458
	TSDT[a]	3.23652	3.08699	2.91168	2.71971	2.52367	2.34345	2.27461
	FSDT[a]	3.23493	3.07586	2.89364	2.6968	2.49698	2.31286	2.2419
	CPT[a]	3.9647	3.71993	3.45164	3.17226	2.89771	2.65182	2.55878
0.8	Present	3.23681	3.14514	3.04268	2.93303	2.81997	2.70848	2.66018
	Ref[a]	3.2372	3.14445	3.04101	2.93052	2.81681	2.74134	2.65659
	SSDT[a]	3.23775	3.14474	3.04107	2.93038	2.8165	2.74092	2.65609
	TSDT[a]	3.23652	3.14431	3.04137	2.93131	2.81794	2.74272	2.65798
	FSDT[a]	3.23493	3.13952	3.03406	2.92193	2.80661	2.72895	2.64315
	CPT[a]	3.9647	3.818	3.66058	3.49712	3.33246	3.21552	3.10423
1	Present	3.23681	3.23681	3.23681	3.23681	3.23681	3.23681	3.23681
	Ref[a]	3.2372	3.2372	3.2372	3.2372	3.2372	3.2372	3.2372
	SSDT[a]	3.23775	3.23775	3.23775	3.23775	3.23775	3.23775	3.23775
	TSDT[a]	3.23652	3.23652	3.23652	3.23652	3.23652	3.23652	3.23652
	FSDT[a]	3.23493	3.23493	3.23493	3.23493	3.23493	3.23493	3.23493
	CPT[a]	3.96470	3.96470	3.96470	3.96470	3.96470	3.96470	3.96470

(a) Kettaf *et al*. (2013)

Table 3 Critical buckling temperature of FG sandwich square plates under linear temperature rise versus gradient index k and t_c/h (a/h=5)

		k						
t_c/h	Theory	0	0.2	0.5	1	2	5	10
0	Present	6.42362	6.09032	5.68966	5.32209	5.20405	5.80773	6.54425
	Ref[(a)]	6.42441	6.09275	5.69414	5.32949	5.21651	5.82957	6.56918
	SSDT[(a)]	6.4255	6.09396	5.69554	5.3313	5.2192	5.83411	6.57458
	TSDT[(a)]	6.42305	6.09084	5.69148	5.32562	5.21036	5.81891	6.5568
	FSDT[(a)]	6.41986	6.04716	5.62014	5.09711	5.09711	5.67452	6.41578
	CPT[(a)]	7.8794	7.28211	6.64118	5.874	5.874	6.60901	7.59882
0.2	Present	6.42362	6.05899	5.60936	5.13228	4.73827	4.64031	4.78400
	Ref[(a)]	6.42441	6.06087	5.61271	5.13775	4.74712	4.65504	4.80264
	SSDT[(a)]	6.4255	6.06197	5.61388	5.13917	4.74907	4.65803	4.80632
	TSDT[(a)]	6.42305	6.05922	5.61059	5.13482	4.74275	4.64797	4.79372
	FSDT[(a)]	6.41986	6.01789	5.5435	5.05105	4.64468	4.52851	4.66058
	CPT[(a)]	7.8794	7.24955	6.55131	5.86076	5.31032	5.14843	5.31369
0.4	Present	6.42362	6.06791	5.63522	5.15892	4.69495	4.34195	4.25879
	Ref[(a)]	6.42441	6.0683	5.63571	5.16024	4.69812	4.34842	4.26735
	SSDT[(a)]	6.4255	6.06913	5.63636	5.16089	4.699	4.34984	4.24818
	TSDT[(a)]	6.42305	6.06734	5.63491	5.15923	4.6964	4.34526	4.26325
	FSDT[(a)]	6.41986	6.03341	5.5799	5.09075	4.61818	4.25591	4.16712
	CPT[(a)]	7.8794	7.28133	6.61708	5.93233	5.29588	4.82217	4.70737
0.5	Present	6.42362	6.09009	5.69067	5.25044	4.80779	4.42714	4.30086
	Ref[(a)]	6.42441	6.08961	5.68948	5.24929	4.8077	4.42943	4.30474
	SSDT[(a)]	6.4255	6.09029	5.68986	5.24952	4.808	4.43011	4.30569
	TSDT[(a)]	6.42305	6.08903	5.68943	5.2494	4.80746	4.42821	4.30281
	FSDT[(a)]	6.41986	6.06053	5.64319	5.19137	4.74084	4.35259	4.22211
	CPT[(a)]	7.8794	7.32529	6.7131	6.07732	5.46601	4.95505	4.78633
0.6	Present	6.42362	6.12545	5.77543	5.39175	4.99943	4.63803	4.49981
	Ref[(a)]	6.42441	6.12425	5.77278	5.38833	4.99619	4.63616	4.49905
	SSDT[(a)]	6.4255	6.12482	5.77291	5.38818	4.99595	4.63609	4.84881
	TSDT[(a)]	6.42305	6.12398	5.77335	5.38942	4.99734	4.6368	4.49922
	FSDT[(a)]	6.41986	6.10171	5.73728	5.34361	4.94396	4.57561	4.43382
	CPT[(a)]	7.8794	7.38985	6.85328	6.29453	5.74542	5.25352	5.06756
0.8	Present	6.42362	6.24028	6.03536	5.81607	5.58995	5.36696	5.27037
	Ref[(a)]	6.42441	6.23889	6.03202	5.81104	5.58362	5.35987	5.26317
	SSDT[(a)]	6.4255	6.23949	6.03215	5.81076	5.58301	5.35923	5.26229
	TSDT[(a)]	6.42305	6.23862	6.03273	5.81262	5.58589	5.36259	5.26598
	FSDT[(a)]	6.41986	6.22905	6.01812	5.79385	5.56322	5.33541	5.2363
	CPT[(a)]	7.8794	7.586	7.27115	6.94424	6.61492	6.29563	6.15846
1	Present	6.42362	6.42362	6.42362	6.42362	6.42362	6.42362	6.42362
	Ref[(a)]	6.42441	6.42441	6.42441	6.42441	6.42441	6.42441	6.42441
	SSDT[(a)]	6.4255	6.4255	6.4255	6.4255	6.4255	6.4255	6.4255
	TSDT[(a)]	6.42305	6.42305	6.42305	6.42305	6.42305	6.42305	6.42305
	FSDT[(a)]	6.41986	6.41986	6.41986	6.41986	6.41986	6.41986	6.41986
	CPT[(a)]	6.42363	6.12545	5.77544	5.39175	4.99944	4.63813	4.49981

(a) Kettaf *et al*. (2013)

Table 4 Critical buckling temperature T_{cr} of FG sandwich square plates under non-linear temperature rise versus gradient index k and t_c/h (a/h=5 and γ=5)

		k						
t_c/h	Theory	0	0.2	0.5	1	2	5	10
0	Present	19.27088	20.56301	21.606477	22.39586	23.00134	23.66406	23.96531
	Ref[(a)]	19.27322	20.57122	21.62347	22.42701	23.05643	23.75304	24.05661
	SSDT[(a)]	19.27655	20.57531	21.62882	22.43468	23.06838	23.77163	24.07624
	TSDT[(a)]	19.26915	20.56479	21.61337	22.41074	23.02926	23.70963	24.01127
	FSDT[(a)]	19.25957	20.41729	21.34246	22.027	22.52869	23.12129	23.49484
	CPT[(a)]	23.6382	24.58692	25.21986	25.60494	25.96247	26.92893	27.8272
0.2	Present	19.27088	20.42384	21.33354	21.97190	22.33166	22.57761	22.76694
	Ref[(a)]	19.27322	20.43016	21.34626	21.99533	22.37338	22.64929	22.85562
	SSDT[(a)]	19.27655	20.43388	21.35077	22.00145	22.38259	22.66392	22.87344
	TSDT[(a)]	19.26915	20.42463	21.33822	21.98279	22.35275	22.61489	22.81317
	FSDT[(a)]	19.25957	20.28528	21.08307	21.62417	21.89055	22.03367	22.17958
	CPT[(a)]	23.6382	24.43703	24.91598	25.09061	25.02775	25.04991	25.2877
0.4	Present	19.27088	20.24425	21.00562	21.53603	21.80468	21.83985	21.83146
	Ref[(a)]	19.27322	20.24553	21.00745	21.54152	21.81937	21.87237	21.87534
	SSDT[(a)]	19.27655	20.2483	21.00993	21.54429	21.82352	21.87961	21.88463
	TSDT[(a)]	19.26915	20.24234	21.00447	21.53734	21.81141	21.85652	21.85429
	FSDT[(a)]	19.25957	20.12913	20.79943	21.25144	21.44811	21.40709	21.36153
	CPT[(a)]	23.6382	24.29255	24.66557	24.76464	24.59556	24.25535	24.13098
0.5	Present	19.27088	20.13367	20.80829	21.28753	21.54826	21.58945	21.55912
	Ref[(a)]	19.27322	20.13209	20.80394	21.28287	21.54783	21.60059	21.57856
	SSDT[(a)]	19.27655	20.13435	20.80531	21.2838	21.54921	21.60389	21.58333
	TSDT[(a)]	19.26915	20.13019	20.80375	21.2833	21.54679	21.59462	21.56887
	FSDT[(a)]	19.25957	20.03597	20.63466	21.04804	21.24818	21.22586	21.16437
	CPT[(a)]	23.6382	24.21722	24.54686	24.64006	24.49836	24.1638	23.99263
0.6	Present	19.27088	20.00566	20.58022	20.99952	21.25335	21.33412	21.32073
	Ref[(a)]	19.27322	20.00176	20.57076	20.98623	21.23955	21.32555	21.31715
	SSDT[(a)]	19.27655	20.00362	20.57125	20.98565	21.23856	21.32526	21.31771
	TSDT[(a)]	19.26915	20.00087	20.5728	20.99045	21.24446	21.32848	21.31794
	FSDT[(a)]	19.25957	19.92815	20.44424	20.81202	21.01752	21.04701	21.00808
	CPT[(a)]	23.6382	24.1352	24.421	24.51562	24.42463	24.16529	24.01085
0.8	Present	19.27087	19.68648	20.00895	20.25624	20.43697	20.55455	20.58763
	Ref[(a)]	19.27322	19.6821	19.99784	20.23872	20.41383	20.5274	20.55953
	SSDT[(a)]	19.27655	19.684	19.99828	20.23774	20.41159	20.5242	20.55608
	TSDT[(a)]	19.26915	19.68124	20.00022	20.24422	20.42213	20.5378	20.5705
	FSDT[(a)]	19.25957	19.65105	19.95177	20.17887	20.33926	20.43371	20.45455
	CPT[(a)]	23.6382	23.9319	24.10594	24.18546	24.18431	24.11121	24.05679
1	Present	19.27087	19.27087	19.27087	19.27087	19.27087	19.27087	19.27087
	Ref[(a)]	19.27322	19.27322	19.27322	19.27322	19.27322	19.27322	19.27322
	SSDT[(a)]	19.27655	19.27655	19.27655	19.27655	19.27655	19.27655	19.27655
	TSDT[(a)]	19.26915	19.26915	19.26915	19.26915	19.26915	19.26915	19.26915
	FSDT[(a)]	19.25957	19.25957	19.25957	19.25957	19.25957	19.25957	19.25957
	CPT[(a)]	23.63820	23.63820	23.63820	23.63820	23.63820	23.63820	23.63820

(a) Kettaf *et al*. (2013)

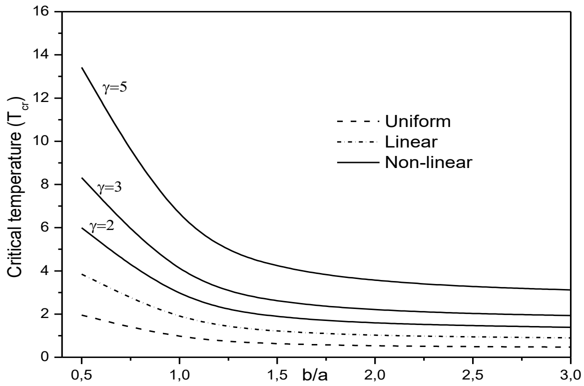

Fig. 5 Critical stability temperature difference T_{cr} of FGM 1 versus the plate aspect ratio *b/a* for FG sandwich square plate with k=1 and t_c=0.8h

While T_{cr} for the plates subjected to a linear temperature variation is intermediate to the two previous thermal loading cases.

Fig. 4 shows the variation of critical temperatures T_{cr} of FG sandwich square plates under to various thermal loading cases with respect to the thickness ratio *a/h*. It can be remarked that with increasing *a/h*, the critical temperature T_{cr} decreases monotonically. Note that in the case of the uniform temperature rise, the critical temperatures T_{cr} of the FG sandwich plate take the smaller values than that of the plate under linear temperature rise and the latter is smaller than that of the plate under non-linear temperature rise. Also, it is observed that T_{cr} increases as the nonlinearity parameter γ increases.

Fig. 5 represents the influences of the aspect ratio *b/a* on the critical stability temperature T_{cr} of FG sandwich subjected to different types of thermal loads. It can be observed that, the critical temperature T_{cr} reduces gradually with increasing the plate aspect ratio *b/a* wherever the thermal loading type. It is also remarked from Fig. 5 that the T_{cr} increases with increasing of the nonlinearity parameter γ.

Fig. 6 demonstrates the effect of thickness of the core t_c on the thermal stability behavior for the FG sandwich square plates under the uniform, linear and nonlinear types of temperature variation within the thickness, respectively. It can be deduced from Figs. 6(a) and (b) (uniform and linear temperature), that the thermal stability temperatures are reduced with increasing the gradient index k. A small values of the gradient index k indicates that the ceramic is the dominant constituent in the FG plate. In addition, it is remarked that the thermal temperatures increase when $t_c \geq 0.4$ which means that the ceramic is also the dominant constituent in the FG plate. As expected, the thermal temperature becomes maximum for the fully ceramic plate (t_c/h=1) in the cases of uniform and linear thermal loads. However, in case of nonlinear thermal load (Fig. 6(c)), the thermal temperature becomes minimum for the fully ceramic plate and the thermal temperatures increase with increasing the gradient index k.

The variation of the critical temperature versus the gradient index k is plotted in Fig. 7(a)-(c) for three different

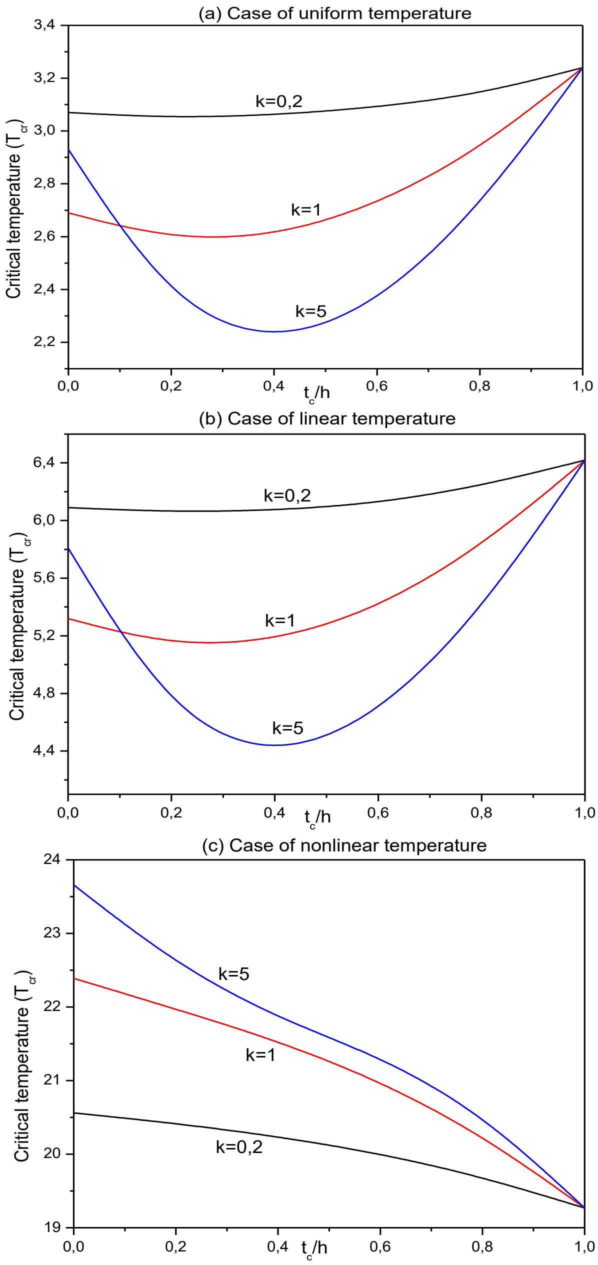

Fig. 6 Critical stability temperature difference T_{cr} of FGM 1 sandwich square plate versus the gradient index k and t_c/h: (a) Uniform temperature; (b) Linear temperature; (c) Nonlinear temperature (γ=5)

FG plates exposed to uniform, linear and nonlinear thermal loads, respectively. It can be concluded from Fig. 7 that the bending stiffness of plates decreases with increase in k values wherever the thermal loading type. This reduction in thermal buckling temperature of FG sandwich plates could be attributed to the metal property. In all considered cases of thermal loading, the stiffness exhibited by FGM 2 sandwich plate is the highest.

The critical buckling temperature versus the thickness of the core layer ratio (t_c/h) plots in non-dimensional T_{cr}-t_c/h plane is presented in Fig. 8(a)-(c). In each of the figures, thermal buckling behavior is shown for FGM 1, FGM 2

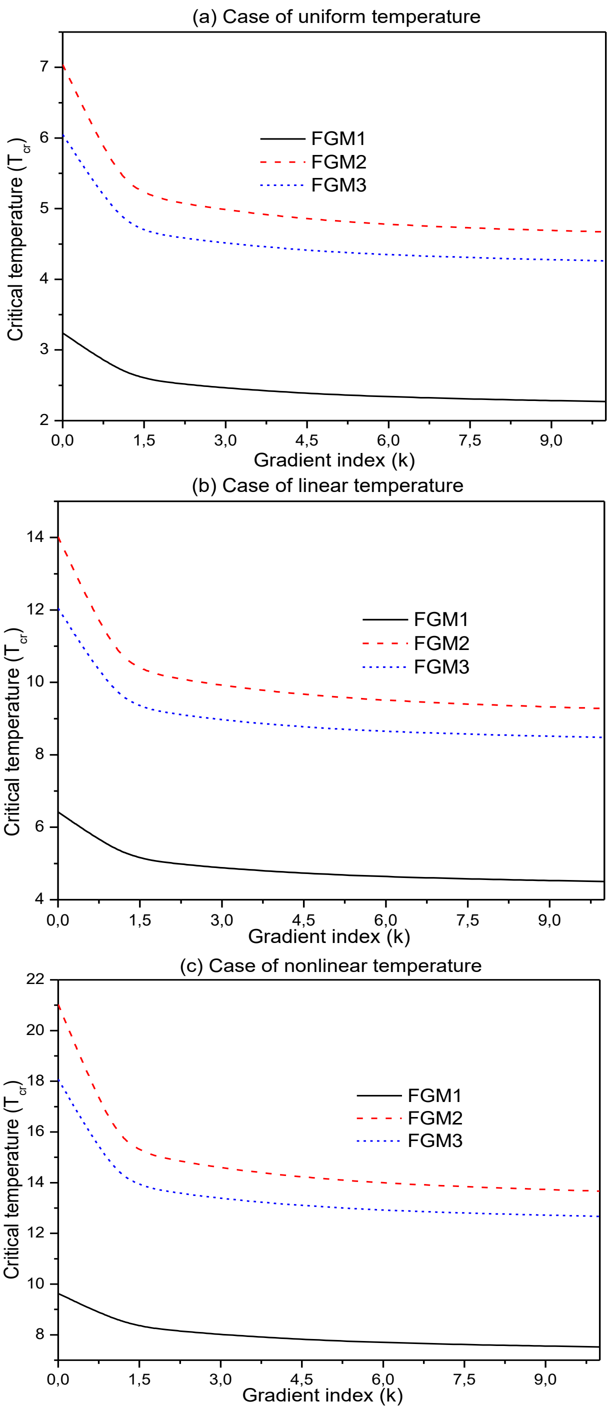

Fig. 7 Critical stability temperature difference T_{cr} of FGM 1, FGM 2 and FGM 3 sandwich square plates versus the gradient index k with t_c/h=0.6: (a) Uniform temperature; (b) Linear temperature; (c) Nonlinear temperature (γ=2)

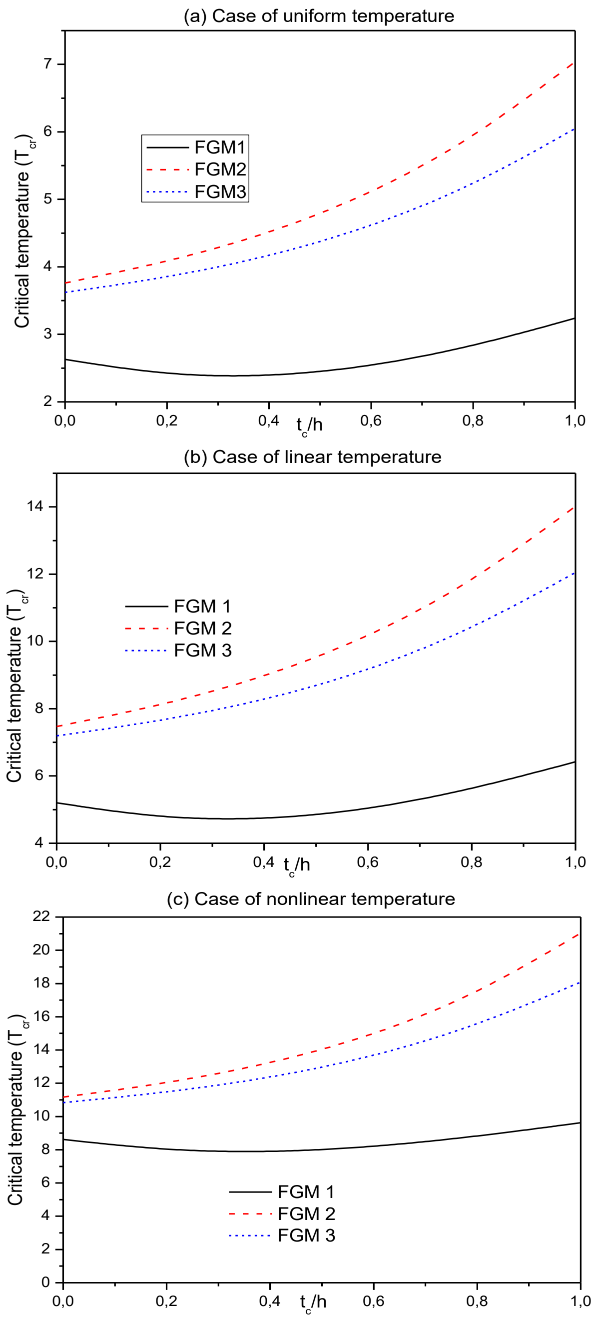

Fig. 8 Critical stability temperature difference T_{cr} of FGM 1, FGM 2 and FGM 3 sandwich square plates versus t_c/h with k=2 and a/h=5: (a) Uniform temperature; (b) Linear temperature; (c) Nonlinear temperature (γ=2)

and FGM 3 plates. In general, the critical buckling temperature is shown to be increasing with increased the thickness (t_c/h) level as a result of enhanced stiffening effect. However, when t_c/h<0.4, the thermal buckling behavior is reversed for FGM 1. Again, in all considered cases of thermal loading, the stiffness exhibited by FGM 2 sandwich plate is the highest.

5. Conclusions

In this article, a new HSDT is developed to examine the thermal stability behaviors of FG sandwich plates subjected to uniform, linear and nonlinear temperature distributions across the thickness. By considering further simplifying suppositions to the existing HSDTs and with the introduction of an undetermined integral term, the number of variables and governing equations of the proposed HSDT are reduced by one, and thus, make this theory simple and efficient to use. The material properties of the sandwich plate faces are assumed to vary according to power law distribution of the volume fraction of the constituents. The governing equations are obtained by using the energy based variational principle and then are solved using Navier's procedure. The accuracy of the proposed theory has been checked for the thermal buckling analysis of FG sandwich plates. All comparison studies demonstrate that the thermal buckling loads obtained by the proposed theory with four unknowns are almost identical with those predicted by other shear deformation theories containing five unknowns. The practical utilities of this theory are: (1) there is no need to use a shear correction factor; (2) the finite element model based on this model will be free from shear locking since the classical plate theory comes out as a special case of the proposed theory; and (3) the theory is simple and time efficient due to involving only four unknowns. In conclusion, it can be said that the proposed model is accurate and efficient in predicting the thermal buckling response of FG sandwich plates.

References

Ait Amar Meziane, M., Abdelaziz, H.H. and Tounsi, A. (2014), "An efficient and simple refined theory for buckling and free vibration of exponentially graded sandwich plates under various boundary conditions", *J. Sandw. Struct. Mater*., **16**(3), 293-318.

Ait Atmane, H., Tounsi, A., Bernard, F. and Mahmoud, S.R. (2015), "A computational shear displacement model for vibrational analysis of functionally graded beams with porosities", *Steel Compos. Struct*., **19**(2), 369-384.

Ait Yahia, S., Ait Atmane, H., Houari, M.S.A. and Tounsi, A. (2015), "Wave propagation in functionally graded plates with porosities using various higher-order shear deformation plate theories", *Struct. Eng. Mech*., **53**(6), 1143-1165.

Akavci, S.S. (2016), "Mechanical behavior of functionally graded sandwich plates on elastic foundation", *Compos. Part B*, **96**, 136-152.

Al-Basyouni, K.S., Tounsi, A. and Mahmoud, S.R. (2015), "Size dependent bending and vibration analysis of functionally graded micro beams based on modified couple stress theory and neutral surface position", *Compos. Struct*., **125**, 621-630.

Attia, A., Tounsi, A., Adda Bedia, E.A. and Mahmoud, S.R. (2015), "Free vibration analysis of functionally graded plates with temperature-dependent properties using various four variable refined plate theories", *Steel Compos. Struct*., **18**(1), 187-212.

Bakora, A. and Tounsi, A. (2015), "Thermo-mechanical post-buckling behavior of thick functionally graded plates resting on elastic foundations", *Struct. Eng. Mech*., **56**(1), 85-106.

Belabed, Z., Houari, M.S.A., Tounsi, A., Mahmoud, S.R. and Anwar Bég, O. (2014), "An efficient and simple higher order shear and normal deformation theory for functionally graded material (FGM) plates", *Compos.: Part B*, **60**, 274-283.

Beldjelili, Y., Tounsi, A. and Mahmoud, S.R. (2016), "Hygro-thermo-mechanical bending of S-FGM plates resting on variable elastic foundations using a four-variable trigonometric plate theory", *Smart Struct. Syst*., **18**(4), 755-786.

Belkorissat, I., Houari, M.S.A., Tounsi, A., Adda Bedia, E.A. and Mahmoud, S.R. (2015), "On vibration properties of functionally graded nano-plate using a new nonlocal refined four variable model", *Steel Compos. Struct*., **18**(4), 1063-1081.

Bellifa, H., Benrahou, K.H., Hadji, L., Houari, M.S.A. and Tounsi, A. (2016), "Bending and free vibration analysis of functionally graded plates using a simple shear deformation theory and the concept the neutral surface position", *J. Braz. Soc. Mech. Sci. Eng*., **38**(1), 265-275.

Bennoun, M., Houari, M.S.A. and Tounsi, A. (2016), "A novel five variable refined plate theory for vibration analysis of functionally graded sandwich plates", *Mech. Adv. Mater. Struct*., **23**(4), 423-431.

Bouderba, B., Houari, M.S.A. and Tounsi, A. (2013), "Thermomechanical bending response of FGM thick plates resting on Winkler-Pasternak elastic foundations", *Steel Compos. Struct*., **14**(1), 85-104.

Bouderba, B., Houari, M.S.A., Tounsi, A. and Mahmoud, S.R. (2016), "Thermal stability of functionally graded sandwich plates using a simple shear deformation theory", *Struct. Eng. Mech*., **58**(3), 397-422.

Boukhari, A., Ait Atmane, H., Tounsi, A., Adda Bedia, E.A. and Mahmoud, S.R. (2016), "An efficient shear deformation theory for wave propagation of functionally graded material plates", *Struct. Eng. Mech*., **57**(5), 837-859.

Bounouara, F., Benrahou, K.H., Belkorissat, I. and Tounsi, A. (2016), "A nonlocal zeroth-order shear deformation theory for free vibration of functionally graded nanoscale plates resting on elastic foundation", *Steel Compos. Struct*., **20**(2), 227-249.

Bourada, M., Kaci, A., Houari, M.S.A. and Tounsi, A. (2015), "A new simple shear and normal deformations theory for functionally graded beams", *Steel Compos. Struct*., **18**(2), 409-423.

Bourada, F., Amara, K. and Tounsi, A. (2016), "Buckling analysis of isotropic and orthotropic plates using a novel four variable refined plate theory", *Steel Compos. Struct*., **21**(6), 1287-1306.

Bousahla, A.A., Benyoucef, S., Tounsi, A. and Mahmoud, S.R. (2016), "On thermal stability of plates with functionally graded coefficient of thermal expansion", *Struct. Eng. Mech*., **60**(2), 313-335.

Bousahla, A.A., Houari, M.S.A., Tounsi, A. and Adda Bedia, E.A. (2014), "A novel higher order shear and normal deformation theory based on neutral surface position for bending analysis of advanced composite plates", *Int. J. Comput. Meth*., **11**(6), 1350082.

Brush, D.O. and Almroth, B.O. (1975), "Buckling of bars, plates, and shells", New York: McGraw-Hill.

Draiche, K., Tounsi, A. and Mahmoud, S.R. (2016), "A refined theory with stretching effect for the flexure analysis of laminated composite plates", *Geomech. Eng*., **11**(5), 671-690

Duc, N.D. and Cong, P.H. (2013), "Nonlinear postbuckling of symmetric S-FGM plates resting on elastic foundations using higher order shear deformation plate theory in thermal environments", *Compos. Struct*., **100**, 566-574.

Fuchiyama, T. and Noda, N. (1995), "Analysis of thermal stress in a plate of functionally gradient material", *JSAE Rev*., **16**(3), 263-268.

Hamidi, A., Houari, M.S.A., Mahmoud, S.R. and Tounsi, A. (2015), "A sinusoidal plate theory with 5-unknowns and stretching effect for thermomechanical bending of functionally graded sandwich plates", *Steel Compos. Struct*., **18**(1), 235-253.

Hebali, H., Tounsi, A., Houari, M.S.A., Bessaim, A. and Adda Bedia, E.A. (2014), "A new quasi-3D hyperbolic shear deformation theory for the static and free vibration analysis of functionally graded plates", *J. Eng. Mech*., ASCE, **140**(2), 374-383.

Houari, M.S.A., Tounsi, A., Bessaim, A. and Mahmoud, S.R. (2016), "A new simple three -unknown sinusoidal shear deformation theory for functionally graded plates", *Steel Compos. Struct*., **22**(2), 257-276.

Houari, M.S.A., Tounsi, A. and Anwar Bég, O. (2013), "Thermoelastic bending analysis of functionally graded sandwich plates using a new higher order shear and normal deformation theory", *Int. J. Mech. Sci*., **76**, 467-479.

Houari, M.S.A, Benyoucef, S., Mechab, I., Tounsi, A. and Adda bedia, E.A. (2011), "Two variable refined plate theory for thermoelastic bending analysis of functionally graded sandwich plates", *J. Therm. Stress.*, **34**(4), 315-334.

Kar, V.R. and Panda, S.K. (2016a), "Nonlinear thermomechanical deformation behaviour of P-FGM shallow spherical shell panel", *Chinese J. Aeronautics*, **29**(1), 173-183.

Kar, V.R., Mahapatra, T.R. and Panda, S.K. (2015), "Nonlinear flexural analysis of laminated composite flat panel under hygro-thermo-mechanical loading", *Steel Compos. Struct*., **19**(4), 1011-1033.

Kar, V.R. and Panda, S.K. (2015a), "Thermoelastic analysis of functionally graded doubly curved shell panels using nonlinear finite element method", *Compos. Struct.*, **129**, 202-212.

Kar, V.R. and Panda, S.K. (2015b), "Large deformation bending analysis of functionally graded spherical shell using FEM", *Struct. Eng. Mech.*, **53**(4), 661-679.

Kar, V.R. and Panda, S.K. (2015c), "Free vibration responses of temperature dependent functionally graded curved panels under thermal environment", *Latin Am. J. Solid. Struct.*, **12**(11), 2006-2024.

Katariya, P.V. and Panda, S.K. (2016), "Thermal buckling and vibration analysis of laminated composite curved shell panel", *Aircraft Eng. Aero. Technol.*, **88**(1), 97-107.

Kar, V.R. and Panda, S.K. (2016b), "Nonlinear thermomechanical behavior of functionally graded material cylindrical/hyperbolic/elliptical shell panel with temperature-dependent and temperature-independent properties", *J. Press. Vessel Technol*., **138**(6), 061202.

Kar, V.R. and Panda, S.K. (2016c), "Post-buckling analysis of shear deformable FG shallow spherical shell panel under uniform and non-uniform thermal environment", *J. Therm. Stress*., **40**(1), 25-39.

Kar, V.R. and Panda, S.K. (2016d), "Post-buckling behaviour of shear deformable functionally graded curved shell panel under edge compression", *Int. J. Mech. Sci*., **115**, 318-324.

Kar, V.R., Mahapatra, T.R. and Panda, S.K. (2016), "Effect of different temperature load on thermal postbuckling behaviour of functionally graded shallow curved shell panels", *Compos. Struct*., **160**, 1236-1247.

Kettaf, F.Z., Houari, M.S.A., Benguediab, M. and Tounsi, A. (2013), "Thermal buckling of functionally graded sandwich plates using a new hyperbolic shear displacement model", *Steel Compos. Struct.*, **15**(4), 399-423.

Laoufi, I., Ameur, M., Zidi, M., Adda Bedia, E.A. and Bousahla, A.A. (2016), "Mechanical and hygrothermal behaviour of functionally graded plates using a hyperbolic shear deformation theory", *Steel Compos. Struct.*, **20**(4), 889-911.

Larbi Chaht, F., Kaci, A., Houari, M.S.A., Tounsi, A., Anwar Bég, O. and Mahmoud, S.R. (2015), "Bending and buckling analyses of functionally graded material (FGM) size-dependent nanoscale beams including the thickness stretching effect", *Steel Compos. Struct*., **18**(2), 425-442.

Liew, K.M., Yang, J. and Kitipornchai, S. (2004), "Thermal post-buckling of laminated plates comprising functionally graded materials with temperature-dependent properties", *J. Appl. Mech. Trans*., ASME, **71**(6), 839-850.

Ma, L.S. and Lee, D.W. (2011), "A further discussion of nonlinear mechanical behavior for FGM beams under in-plane thermal loading", *Compos. Struct.*, **93**(2), 831-842.

Ma, L.S. and Lee, D.W. (2012), "Exact solutions for nonlinear static responses of a shear deformable FGM beam under an in-plane thermal loading", *Euro. J. Mech.-A/Solids*, **31**(1), 13-20.

Mahapatra, T.R., Kar, V.R. and Panda, S.K. (2016a), "Large amplitude vibration analysis of laminated composite spherical panels under hygrothermal environment", *Int. J. Struct. Stability Dyn*., **16**(3), 1450105.

Mahapatra, T.R., Panda, S.K. and Kar, V.R. (2016b), "Nonlinear hygro-thermo-elastic vibration analysis of doubly curved composite shell panel using finite element micromechanical model", *Mech. Adv. Mater. Struct*., **23**(11), 1343-1359.

Mahapatra, T.R., Kar, V.R. and Panda, S.K. (2016c), "Large amplitude bending behaviour of laminated composite curved panels", *Eng. Comput*., **33**(1), 116-138.

Mahapatra, T.R., Panda, S.K. and Kar, V.R. (2016d), "Nonlinear flexural analysis of laminated composite panel under hygro-thermo-mechanical loading: A micromechanical approach", *Int. J. Comput. Meth*., **13**(3), 1650015.

Mahapatra, T.R., Panda, S.K. and Kar, V.R. (2016e), "Geometrically nonlinear flexural analysis of hygro-thermo-elastic laminated composite doubly curved shell panel", *Int. J. Mech. Mater. Des*., **12**(2), 153-171.

Mahapatra, T.R., Kar, V.R. and Panda, S.K. (2016f), "Nonlinear free vibration analysis of laminated composite doubly curved shell panel in hygrothermal environment", *J. Sandw. Struct. Mater*., **17**(5), 511-545.

Mahapatra, T.R. and Panda, S.K. (2015), "Thermoelastic vibration analysis of laminated doubly curved shallow panels using non-linear FEM", *J. Therm. Stress*., **38**(1), 39-68.

Mahapatra, T.R. and Panda, S.K. (2016), "Nonlinear free vibration analysis of laminated composite spherical shell panel under elevated hygrothermal environment: A micromechanical approach", *Aerosp. Sci. Technol*., **49**, 276-288.

Mahi, A., Adda Bedia, E.A. and Tounsi, A. (2015), "A new hyperbolic shear deformation theory for bending and free vibration analysis of isotropic, functionally graded, sandwich and laminated composite plates", *Appl. Math. Model*., **39**, 2489-2508.

Matsunaga, H. (2009), "Thermal buckling of functionally graded plates according to a 2 D higher-order deformation theory", *Compos. Struct.*, **90**(1), 76-86.

Mehar, K. and Panda, S.K. (2016a), "Geometrical nonlinear free vibration analysis of FG-CNT reinforced composite flat panel under uniform thermal field", *Compos. Struct*., **143**, 336-346.

Mehar, K. and Panda, S.K. (2016b), "Thermoelastic analysis of FG-CNT reinforced shear deformable composite plate under various loadings", *Int. J. Comput. Method*., 1750019.

Mehar, K., Panda, S.K., Dehengia, A. and Kar, V.R. (2016), "Vibration analysis of functionally graded carbon nanotube reinforced composite plate in thermal environment", *J. Sandw. Struct. Mater*., **18**(2), 151-173.

Mehar, K. and Panda, S.K. (2017), "Numerical investigation of nonlinear thermomechanical deflection of functionally graded CNT reinforced doubly curved composite shell panel under different mechanical loads", *Compos. Struct*., **161**, 287-298.

Meksi, A., Benyoucef, S., Houari, M.S.A. and Tounsi, A. (2015), "A simple shear deformation theory based on neutral surface position for functionally graded plates resting on Pasternak elastic foundations", *Struct. Eng. Mech*., **53**(6), 1215-1240.

Meradjah, M., Kaci, A., Houari, M.S.A., Tounsi, A. and Mahmoud, S.R. (2015), "A new higher order shear and normal deformation theory for functionally graded beams", *Steel Compos. Struct*., **18**(3), 793-809.

Meyers, C.A. and Hyer, M.W. (1991), "Thermal buckling and postbuckling of symmetrically laminated composite plates", *J. Therm. Stress*., **14**(4), 519-540.

Na, K.S. and Kim, J.H. (2006), "Three-dimensional thermomechanical buckling analysis for functionally graded composite plates", *Compos. Struct*., **73**(4), 413-422.

Nguyen, K.T., Thai, T.H. and Vo, T.P. (2015), "A refined higher-order shear deformation theory for bending, vibration and buckling analysis of functionally graded sandwich plates", *Steel Compos. Struct.*, **18**(1), 91-120.

Panda, S.K. and Singh, B.N. (2009), "Thermal post-buckling behaviour of laminated composite cylindrical/hyperboloid shallow shell panel using nonlinear finite element method", *Compos. Struct.*, **91**(3), 366-374.

Panda, S.K. and Singh, B.N. (2013a), "Post-buckling analysis of laminated composite doubly curved panel embedded with SMA fibers subjected to thermal environment", *Mech. Adv. Mater. Struct.*, **20**(10), 842-853.

Panda, S.K. and Singh, B.N. (2013b), "Thermal postbuckling behavior of laminated composite spherical shell panel using NFEM", *Mech. Based Des. Struct. Machines*, **41**(4), 468-488.

Panda, S.K. and Singh, B.N. (2013c), "Nonlinear finite element analysis of thermal post-buckling vibration of laminated composite shell panel embedded with SMA fibre", *Aerosp. Sci. Technol.*, **29**(1), 47-57.

Panda, S.K. and Singh, B.N. (2013d), "Large amplitude free vibration analysis of thermally post-buckled composite doubly curved panel embedded with SMA fibers", *Nonlinear Dyn.*, 74(1), 395-418.

Panda, S.K. and Singh, B.N. (2011), "Large amplitude free vibration analysis of thermally post-buckled composite doubly curved panel using nonlinear FEM", *Finite Element. Anal. Des*, **47**(4), 378-386.

Panda, S.K. and Singh, B.N. (2010a), "Thermal post-buckling analysis of a laminated composite spherical shell panel embedded with shape memory alloy fibres using non-linear finite element method", *Proceeding of the IMechE Part C: Journal of Mechanical Engineering and Science*, **224**(4), 757-769.

Panda, S.K. and Singh, B.N. (2010b), "Nonlinear free vibration analysis of thermally post-buckled composite spherical shell panel", *Int. J. Mech. Mater. Des.*, **6**(2), 175-188.

Panda, S.K. and Katariya, P.V. (2015), "Stability and free vibration behaviour of laminated composite panels under thermo-mechanical loading", *Int. J. Appl. Comput. Math.*, **1**(3), 475-490.

Piovan, M.T. and Machado, S.P. (2011), "Thermoelastic dynamic stability of thin-walled beams with graded material properties", *Thin Wall. Struct.*, **49**(3), 437-447.

Reddy, J.N. (1984), *Energy principles and variational methods in applied mechanics*, New York: John Wiley.

Singh, V.K. and Panda, S.K. (2015), "Large amplitude free vibration analysis of laminated composite spherical shells embedded with piezoelectric layers", *Smart Struct. Syst.*, **16**(5), 853-872.

Tounsi, A., Houari, M.S.A., Benyoucef, S. and Adda Bedia, E.A. (2013), "A refined trigonometric shear deformation theory for thermoelastic bending of functionally graded sandwich plates", *Aerosp. Sci. Technol.*, **24**(1), 209-220.

Tounsi, A., Houari, M.S.A. and Bessaim, A. (2016), "A new 3-unknowns non-polynomial plate theory for buckling and vibration of functionally graded sandwich plate", *Struct. Eng. Mech.*, **60**(4), 547-565.

Zhao, X., Lee, Y.Y. and Liew, K.M. (2009), "Mechanical and thermal buckling analysis of functionally graded plates", *Compos. Struct.*, **90**(2), 161-171.

Zidi, M., Tounsi, A., Houari M.S.A., Adda Bedia, E.A. and Anwar Bég, O. (2014), "Bending analysis of FGM plates under hygro-thermo-mechanical loading using a four variable refined plate theory", *Aerosp. Sci. Technol.*, **34**, 24-34.

CC